International Journal of Mechanical Sciences 165 (2020) 105211

Contents lists available at ScienceDirect

International Journal of Mechanical Sciences

journal homepage: www.elsevier.com/locate/ijmecsci

Thermoelastic damping in micro and nano-mechanical resonators utilizing entropy generation approach and heat conduction model with a single delay term

Harendra Kumar*, Santwana Mukhopadhyay

Department of Mathematical Sciences, Indian Institute of Technology (BHU), Varanasi, India

A R T I C L E I N F O

Keywords:
Thermoelastic damping
Entropy
Micro/nano-beam resonator
Time delay parameter
Non-Fourier effects

A B S T R A C T

Analysis of thermoelastic damping (TED) of micro and nano-beam resonators plays a very important role in designing the resonator with high-quality factors. TED of micro and nano-beam resonators has therefore been an interesting and challenging area of research in recent years. Prediction of TED is more challenging under the effect of non-Fourier heat conduction. In the past, several works have been dedicated to TED modeling with the influence of non-Fourier heat conduction in view of the fact that non-Fourier heat conduction model is more relevant for analysis of TED for small scale devices. The present work aims to investigate TED in micro and nano-mechanical resonators utilizing non-Fourier heat conduction model with a single delay term introduced by Quintanilla in 2011. We derive an explicit formula of the quality factor for TED based on the entropy generation approach. With the help of numerical results, we present the influence of TED in the context of normalized frequency as well as beam thickness. Further, the effects of the time delay parameter and the material constants on TED have been discussed in detail. The results of the present model are compared to those obtained for GN-III model. It has been observed that the current model offers a high-quality factor as compared to GN-III model.

1. Introduction

Thermoelastic damping (TED) is a major source of internal damping in micro-electromechanical systems (MEMS) and nano-electromechanical systems (NEMS) working under vacuum condition. MEMS/NEMS are widely used in engineering and science due to their applications such as signal processing filters, sensors, micro-actuators, microscopes, etc., where the high-quality factors are required [1,2]. One of the popular applications of MEMS/NEMS devices is micro/nano-beam resonators. The quality factor (Q-factor) is used to measure the quality performance of the resonators. The Q-factor is defined as the ratio of the stored energy in the system to the energy dissipated by the system for various damping mechanisms per cycle of vibrations. The dissipation effects are generally measured by Q-factor during the vibrations. The high Q-factor of a resonator indicates the lower rate of energy dissipation and implying its higher sensitivity. Generally, the dissipation of energy of the systems can be classified into two groups, internal loss and external loss. Among energy dissipation mechanisms for a large range of micro and nano-mechanical resonators, TED is considered more important than other damping factors [3,4]. The accurate Q-factor prediction is important to design the high-performance of micro and nano-mechanical devices. There are some methods developed for Q-factor prediction due to TED. One of these methods, the most adopted one is complex-frequency approach method [5], where the Q-factor is given by $Q^{-1} = 2|Im(\omega)/Re(\omega)|$,where ω is in general considered as complex-frequency. Here, $Im(\omega)$ and $Re(\omega)$ indicate the imaginary and real part of ω, which gives the attenuation of the vibration and the new eigen-frequencies in the presence of TED, respectively. Other methods are thermal-energy method (entropy generation approach) [6], the finite element-based method [7], and molecular dynamics simulation method [8,9].

In 1937 and 1938, Zener [10,11] first developed an analytical model for TED in a vibrating beam. Here, the heat conduction was considered only along the cross-section of the beam. In 1990, Green and Naghdi [12–14] established different thermoelastic models, which are known as GN-I, GN-II, and GN-III models. The work of Zener had been improved by Lifshitz and Roukes [5] in 2000, developing precise and closed-form expression for TED. The flexural vibrations in a thermoelastic body produce an oscillating stress gradient and an oscillating temperature gradient, which is caused by the coupling of the strain field and the temperature field. The temperature gradient essentially increases the flow of heat from the higher temperature to the lower temperature regimes. This energy dissipation process is termed as TED. Due to the effects of irreversible heat flow, the thermal strain field result in fluctuating temperature is out of phase with the applied stress field for the vi-

* Corresponding author.
E-mail address: harendra.rs.mat16@iitbhu.ac.in (H. Kumar).

https://doi.org/10.1016/j.ijmecsci.2019.105211
Received 20 April 2019; Received in revised form 2 October 2019; Accepted 3 October 2019
Available online 7 October 2019
0020-7403/

brating resonators. This phase difference accounts for the conversion of mechanical energy into heat. As per the second law of thermodynamics, this heat flow can produce entropy, which appears as conservation of useful mechanical energy into heat. This process of entropy generation is used in the analysis of TED by the entropy generation method. In 1994, Kinra and Milligan [15] analyzed TED based on the second law of thermodynamics and established a general theory for calculating TED from the entropy produced. Later on, there are many researchers who analyzed TED in MEMS resonators based on this concept of entropy generation [16–18]. Khisaeva and Ostoja-Starzewski [19] studied the associated TED in micro-beam resonators considering generalized thermoelasticity theory with one relaxation time. They have used the approach of Kinra and Milligan [15] considering a starting point and the difference between temperature distribution across the beam thickness between classical and nonclassical theory for a broad frequency range. Bostani and Mohammadi [20] investigated the behavior of TED in beam resonators using modified strain gradient elasticity as well as generalized thermoelasticity theories. Guo et al.[21] studied the nature of vibrations of TED in micro-beam resonators at the nanoscale utilizing the generalized thermoelasticity theory with the dual-phase-lags (DPL) thermal conduction model. The DPL heat conduction model is a modification of Fourier law proposed by Tzou [22] by defining two different phase lag parameters of the heat flux vector and the thermal gradient vector. Kumar et al. [23] estimated TED in micro-mechanical resonators on the basis of the three-phase-lag (TPL) heat conduction model. This model modified by Roychoudhuri [24] is an extension of Tzou's heat conduction model containing one more relaxation time of thermal displacement vector, which is different from the heat flux vector and thermal gradient vector associated with DPL heat conduction model.

In recent years, some investigations dealing with the TED in beams and plates have been reported (see Refs. [25–46]). Analysis of TED considering ring structures can be found in the articles [47–53]. We refer to some useful investigations [54–63] on thermoelastic vibration of beams and plates considering the modified couple stress theory. Recently, Kumar et al. [64] analyzed TED in micro-beam resonator, considering thermoelasticity theory with a single delay term introduced by Quintanilla [65]. They adopted complex-frequency approach and derived a more general formula of the inverse quality factor by considering the thermoelasticity theories of type TPL, LS, GN-III, and thermoelasticity theory with a single delay term in a unified way. In their work, it is found that the quality factor under thermoelasticity theory with a single delay term is greater than that under TPL and LS theories while agrees with the results by GN-III theory.

The main contribution of the present work is to present a generalized model to accurately capture the TED in beam resonator at micro and nanoscale structures by employing the non-Fourier heat conduction model with a single delay term proposed by Quintanilla [65]. We present the entropy-based method to estimate TED and give an explicit analytical formula of the quality factor due to TED. The results of the present model are compared with those obtained for GN-III model. There is a lack of the experimental value of some material constants associated with the non-Fourier heat conduction equation to accurately capture the TED in MEMS/NEMS resonators, sometimes hypothetical values of some parameters are assumed by researchers. In this work, we obtain the results by considering three different cases in the value of thermal conductivity rate that is a material constant characteristic of the GN-III model and the present model. We analyze our results for the cases when this material constant is greater than the thermal conductivity, equal to the thermal conductivity, and less than the thermal conductivity by assuming the thermal conductivity of the material associated with the heat conduction equation is known. We highlight the differences in predictions of the quality factor for all three cases. The obtained results can help the researchers for calculating TED accurately in micro and nano-beam resonators based on the present modified Fourier law. It is also believed that the present investigation will bring to light a detailed understanding of TED analysis under the influence of the present model and GN-III model.

2. Problem formulation

In this article, we consider a non-Fourier heat conduction equation with a single delay term suggested by Quintanilla [65]. This heat conduction equation is developed as a reformulation of TPL heat conduction model (Roychoudhuri [24]) by introducing a delay term between heat flux vector and thermal displacement vector with the assumption that the phase lag of heat flux vector is equal to the phase lag of the thermal gradient vector (i.e., $\tau = \tau_q - \tau_v$ and $\tau_q = \tau_T$). Here, the term τ_q that results the small scale effects of heat transport in space such as phonon scattering or phonon-electron interaction, is called the phase lag of heat flux. The term τ_T results from the rapid transient effects of thermal inertia, is called the phase lag of thermal gradient [22]. The term τ_v is termed as the phase lag of the thermal displacement gradient [24]. The non-Fourier heat conduction equation with a single delay term introduced by Quintanilla [65] is given by

$$q_i(r,t) = -\left[kT,_i(r,t) + k^* \upsilon,_i(r,t-\tau)\right] \tag{1}$$

where $\dot{\upsilon} = T$. In the above equation, q indicates the heat flux vector, T the temperature, r the position vector, k^* the material constant characteristic of the theory, k the thermal conductivity of the material, and υ indicates the thermal displacement vector. Expanding Eq. (1) upto second order in τ by Taylor series expansion, one can obtain

$$q_i = -\left[\left(k - k^*\tau\right)T,_i + \frac{\tau^2 k^*}{2}\dot{T},_i + k^*\upsilon,_i\right] \tag{2}$$

The heat flux, temperature, and dilatation strain due to the thermal effect of thermoelastic isotropic material is defined as [66]

$$-q_{i,i} = \rho C_v \frac{\partial T}{\partial t} + \frac{TE\alpha_T}{(1-2\nu)}\frac{\partial e}{\partial t} \tag{3}$$

where ρ indicates the mass density, C_v the specific heat capacity at constant volume, ν the Poisson's ratio, α_T the thermal expansion coefficient, and e indicates the dilatation strain. By using Eqs. (2) and (3) in view of $\dot{\upsilon} = T$, we get

$$k^*T,_{ii} + \left(k - k^*\tau\right)\dot{T},_{ii} + \frac{\tau^2 k^*}{2}\ddot{T},_i = \rho C_v \ddot{T} + \frac{TE\alpha_T}{(1-2\nu)}\ddot{e} \tag{4}$$

The above equation further can be rewritten in the following form:

$$k^*\theta,_{ii} + \left(k - k^*\tau\right)\dot{\theta},_{ii} + \frac{\tau^2 k^*}{2}\ddot{\theta},_i = \rho C_v \ddot{\theta} + \frac{T_0 E\alpha_T}{(1-2\nu)}\ddot{e} \tag{5}$$

where $\theta = T - T_0$ is change in temperature from the reference temperature T_0. It is worth noting that when $\tau = 0$, the present thermoelasticity model recovers the thermoelasticity theory of type GN-III.

3. TED in micro and nano-beam resonators

In this section, we consider a thin elastic beam (Euler–Bernoulli beam) with small flexural deflection of length L with a rectangular cross-section of dimension $h \times b$ as shown in Fig. 1, assuming the x−axis along the axis of the beam, y−axis along the thickness of the beam, and z−axis along the width of the beam. In the equilibrium, it is considered that the beam is unstrained, unstressed, and kept at uniform temperature T_0 everywhere. Therefore, the strain tensor and dilatation strain are given by [5,66]

$$\varepsilon_{11} = -y\frac{\partial^2 w}{\partial x^2},\ \ \varepsilon_{22} = \varepsilon_{33} = \nu y\frac{\partial^2 w}{\partial x^2} + (1+\nu)\alpha_T\theta$$

$$e = \varepsilon_{11} + \varepsilon_{22} + \varepsilon_{33} = (2\nu - 1)y\frac{\partial^2 w}{\partial x^2} + 2(1+\nu)\alpha_T\theta \tag{6}$$

where w represents the deflection of the beam. Inserting Eq. (6) into Eq. (5), one can obtain

$$\left[\frac{k^*}{k}\left(1 - \tau\frac{\partial}{\partial t} + \frac{\tau^2}{2}\frac{\partial^2}{\partial t^2}\right) + \frac{\partial}{\partial t}\right]\theta,_{ii} = \frac{1}{\chi}\left(\Omega\ddot{\theta} - \frac{\Delta_E y}{\alpha_T}\frac{\partial^4 w}{\partial t^2 \partial x^2}\right) \tag{7}$$

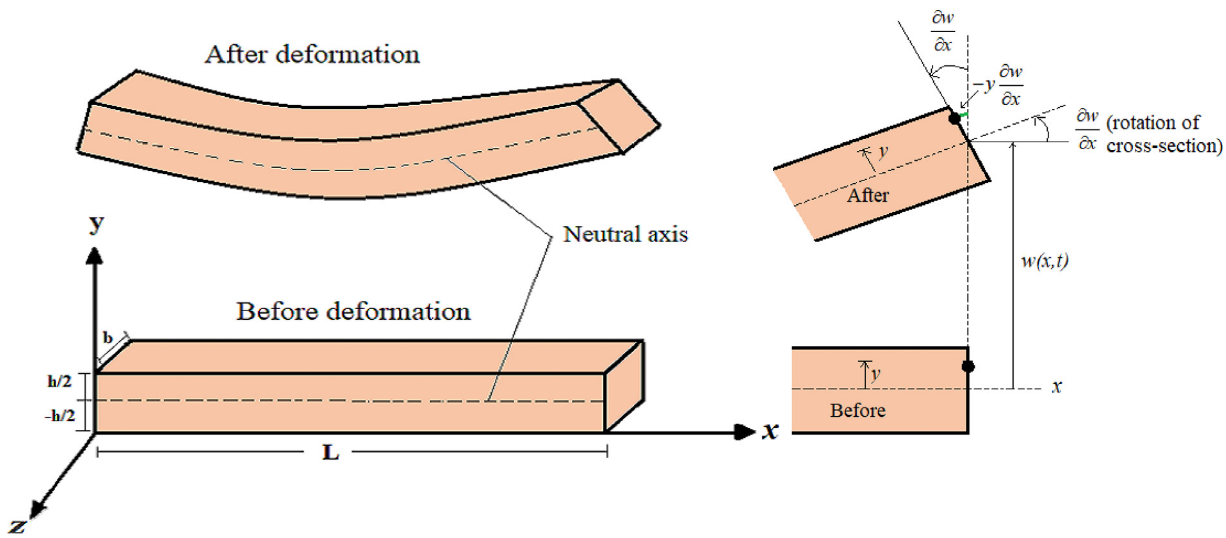

Fig. 1. Deformation of an Euler–Bernoulli beam.

where $\Omega = \frac{(1-2\nu)+2\Delta_E(1+\nu)}{(1-2\nu)}$, $\chi = \frac{k}{\rho C_v}$ indicates the thermal diffusivity of the material, and $\Delta_E = \frac{E\alpha_T^2 T_0}{\rho C_v}$ represents the relaxation strength of Young's modulus (the relative difference between the adiabatic and isothermal values of Young's modulus). It can be noted that Δ_E is dimensionless and $\Delta_E \ll 1$. It is further worth noting that thermal gradients in the cross-section of the plane along the y−direction are much larger than the gradients along the axis of beam and no gradient exists in the direction of z−axis. Therefore replacing $\theta,_{ii}$ by $\frac{\partial^2\theta}{\partial y^2}$ in Eq. (7), we obtain

$$\left[\frac{k^*}{k}\left(1-\tau\frac{\partial}{\partial t}+\frac{\tau^2}{2}\frac{\partial^2}{\partial t^2}\right)+\frac{\partial}{\partial t}\right]\frac{\partial^2\theta}{\partial y^2} = \frac{1}{\chi}\left(\Omega\ddot{\theta} - \frac{\Delta_E y}{\alpha_T}\frac{\partial^4 w}{\partial t^2 \partial x^2}\right) \tag{8}$$

4. Solution for harmonic vibration

To find the influence of thermoelastic coupling on harmonic vibrations of the beam resonator, the heat conduction equation Eq. (8) is solved for the case of harmonic vibrations. Firstly, it is assumed that

$$w(x,t) = W(x)e^{i\omega t}, \quad \theta(x,y,t) = \theta_0(x,y)e^{i\omega t} \tag{9}$$

where $W(x)$ denotes the displacement function, $\theta_0(x,\ y)$ denotes a complex-valued function indicating that the temperature field is out of phase with the applied stress, and ω represents the angular frequency of vibration. Substituting Eq. (9) into Eq. (8), we get

$$\left[\frac{k^*}{k}\left(1-i\omega-\frac{\tau^2}{2}\omega^2\right)+i\omega\right]\frac{\partial^2\theta_0}{\partial y^2} = \frac{\omega^2}{\chi}\left(-\Omega\theta_0 + \frac{\Delta_E y}{\alpha_T}\frac{\partial^2 W}{\partial x^2}\right)$$

$$\frac{\partial^2\theta_0}{\partial y^2} = -\frac{\omega^2}{\chi\left[\frac{k^*}{k}\left(1-\frac{\tau^2}{2}\omega^2\right)+i\omega\left(1-\frac{k^*\tau}{k}\right)\right]}\left(\Omega\theta_0 - \frac{\Delta_E y}{\alpha_T}\frac{\partial^2 W}{\partial x^2}\right) \tag{10}$$

The general solution of the above equation can be obtained in the following form:

$$\theta_0(x,y) = D_1 sin(py) + D_2 cos(py) + \frac{\Delta_E y}{\Omega\alpha_T}\frac{\partial^2 W}{\partial x^2} \tag{11}$$

where the unknown coefficients D_1 and D_2 are determined by applying thermal boundary conditions, and p can be expressed as:

$$p = \sqrt{\frac{\omega}{\chi}}\sqrt{a_1 - ia_2} = \frac{\xi\zeta}{h} - i\frac{\xi}{h\zeta}a_2,\ \xi = h\sqrt{\frac{\omega}{2\chi}},\ \zeta = \sqrt{a_1+\sqrt{a_1^2+a_2^2}}$$

$$a_1 = \frac{\Omega\frac{k^*}{k}\left(1-\frac{\tau^2}{2}\omega^2\right)\omega}{\left[\frac{k^*}{k}\left(1-\frac{\tau^2}{2}\omega^2\right)\right]^2+\left[\left(1-\frac{k^*\tau}{k}\right)\omega\right]^2}$$

$$a_2 = \frac{\Omega\left(1-\frac{k^*\tau}{k}\right)\omega^2}{\left[\frac{k^*}{k}\left(1-\frac{\tau^2}{2}\omega^2\right)\right]^2+\left[\left(1-\frac{k^*\tau}{k}\right)\omega\right]^2}$$

The thermal boundary conditions are taken such that the lower and upper surfaces of the beam are adiabatic. In this case, we have

$$\frac{\partial\theta}{\partial y} = 0 \quad at \quad y = \pm\frac{h}{2} \tag{12}$$

Finally, in view of Eqs. (11) and (12), the temperature field function is obtained as:

$$\theta_0(x,y) = \frac{\Delta_E}{\Omega\alpha_T}\frac{\partial^2 W}{\partial x^2}\left[y - \frac{sin(py)}{p\,cos\left(\frac{ph}{2}\right)}\right] \tag{13}$$

5. Entropy based method for TED

The inverse of the quality factor can be defined in terms of energy loss and maximum stored energy per cycle of vibration as [11]

$$Q^{-1} = \frac{1}{2\pi}\frac{\Delta W}{W_{stored}} \tag{14}$$

where ΔW denotes the energy loss and W_{stored} denotes the maximum stored energy, respectively during one period of oscillation. Now, we aim to calculate the lost energy and the maximum stored energy during one period of oscillation. Firstly, the solution of Eq. (8) can be rewritten in the form of temperature field function as:

$$\theta(x,y,t) = \theta_0(x,y)sin(\omega t) \tag{15}$$

Here, ω is a real valued involved in the forced harmonic vibration with no attenuation during one period. From the second law of thermodynamic, the rate of entropy generation per unit volume is expressed as [67]

$$\dot{s} = -\frac{1}{T^2}q_i T,_i \tag{16}$$

For simplification of this equation, when $\theta \ll 1$, the zeroth order term of the Taylor series expansion of T^{-2} around T_0 is considered as:

$$\frac{1}{T^2} = \frac{1}{T_0^2} - O\left(\frac{2}{T_0^3}\theta\right) \tag{17}$$

Hence, substituting the values of q_i from Eq. (16) into Eq. (1) and then using Eq. (17), we arrive at the relation

$$\ddot{s} + \left(\frac{2\dot{T}}{T_0} - \frac{\dot{T}_{,i}}{T_{,i}}\right)\dot{s} = \left[k^* + (k - k^*\tau)\frac{\partial}{\partial t} + \frac{\tau^2 k^*}{2}\frac{\partial^2}{\partial t^2}\right]\frac{(T_{,i})^2}{T_0^2} \tag{18}$$

Since, the term $\frac{2\dot{T}}{T_0}$ is small, hence for mathematical simplicity neglecting this term in Eq. (18), therefore the solution of Eq. (18) for $\dot{s}$ is acquired as:

$$\dot{s} = \frac{1}{T_0^2}\left(\frac{\partial\theta_0}{\partial y}\right)^2\left[\left(\frac{k - k^*\tau}{\omega^2}\right)sin^2(\omega t) - \frac{k^*}{2\omega}\left(1 - \frac{\tau^2}{2\omega^2}\right)sin(2\omega t)\right] \tag{19}$$

Inserting Eq. (13) into Eq. (19), one can obtain

$$\dot{s} = \frac{1}{T_0^2}\left(\frac{\Delta_E}{\Omega\alpha_T}\frac{\partial^2 W}{\partial x^2}\right)^2\left[1 - \frac{cos(py)}{cos\left(\frac{ph}{2}\right)}\right]^2\left\{\sin^2(\omega t) - \frac{k^*}{k}\frac{sin(2\omega t)}{2\omega}\right\} \tag{20}$$

The generation of entropy per unit volume over one cycle of vibration is given by

$$\Delta s = \oint \dot{s}dt \tag{21}$$

By using Eqs. (20) and (21), we obtain

$$\Delta s = \frac{\pi}{\omega^3}\frac{(k - k^*\tau)}{T_0^2}\left(\frac{\Delta_E}{\Omega\alpha_T}\frac{\partial^2 W}{\partial x^2}\right)^2\left[1 - \frac{cos(py)}{cos\left(\frac{ph}{2}\right)}\right]^2 \tag{22}$$

We can obtain the total entropy production over one cycle by integrating Eq. (22) over the volume of the beam as follows:

$$\Delta S = \int_V \Delta s dV \tag{23}$$

Substituting Eq. (22) into Eq. (23), we find the following expression

$$\Delta S = \frac{\pi}{\omega^3}\frac{(k - k^*\tau)\Delta_E^2 h}{\alpha_T^2 T_0^2 \Omega^2}A.B = \frac{\pi\left(1 - \frac{k^*\tau}{k}\right)h^3 E\Delta_E}{2\Omega^2 T_0\xi^2}A.B \tag{24}$$

where A and B are the complex functions given by

$$A = \int_{-\frac{h}{2}}^{+\frac{h}{2}}\left[1 + \frac{cos^2(py)}{cos^2\left(\frac{ph}{2}\right)} - \frac{2cos(py)}{cos\left(\frac{ph}{2}\right)}\right]dy = 1 + \frac{1}{1 + cos(ph)} - \frac{3}{ph}tan\left(\frac{ph}{2}\right) \tag{25}$$

$$B = \int_0^L \int_{-\frac{b}{2}}^{+\frac{b}{2}}\left(\frac{\partial^2 W}{\partial x^2}\right)^2 dzdx = b\int_0^L\left(\frac{\partial^2 W}{\partial x^2}\right)^2 dx \tag{26}$$

The real and imaginary parts of Eq. (25) can be separated in view of $p = \frac{\xi\zeta}{h} - i\frac{\xi}{h\zeta}a_2$ as follows:

$$Re(A) = 1 + \frac{1 + cos(\xi\zeta)cosh\left(\frac{\xi a_2}{\zeta}\right)}{\left[cos(\xi\zeta) + cosh\left(\frac{\xi a_2}{\zeta}\right)\right]^2} - \frac{3\zeta\left(\zeta^2 sin(\xi\zeta) + a_2 sinh\left(\frac{\xi a_2}{\zeta}\right)\right)}{\xi\left(\zeta^4 + a_2^2\right)\left[cos(\xi\zeta) + cosh\left(\frac{\xi a_2}{\zeta}\right)\right]}$$

$$Im(A) = -\frac{sin(\xi\zeta)sinh\left(\frac{\xi a_2}{\zeta}\right)}{\left[cos(\xi\zeta) + cosh\left(\frac{\xi a_2}{\zeta}\right)\right]^2} - \frac{3\zeta\left(a_2 sin(\xi\zeta) - \zeta^2 sinh\left(\frac{\xi a_2}{\zeta}\right)\right)}{\xi\left(\zeta^4 + a_2^2\right)\left[cos(\xi\zeta) + cosh\left(\frac{\xi a_2}{\zeta}\right)\right]}$$

Therefore, the total dissipated energy ΔW can be calculated as:

$$\Delta W = T_0|\Delta S| = \frac{\pi\left(1 - \frac{k^*\tau}{k}\right)h^3 E\Delta_E B}{2\Omega^2\xi^2}\sqrt{Re(A)^2 + Im(A)^2} \tag{27}$$

Further, the maximum stored energy W_{stored} over entire beam per cycle is given by

$$W_{stored} = \frac{1}{2}\int_V \sigma_{xx}\epsilon_{xx}dV \tag{28}$$

where $\sigma_{xx} = E\epsilon_{xx}$. Therefore, the maximum stored energy from above equation is obtained as:

$$W_{stored} = \frac{Ebh^3}{24}\int_0^L\left(\frac{\partial^2 W}{\partial x^2}\right)^2 dx = \frac{Eh^3 B}{24} \tag{29}$$

Now, using Eqs. (27) and (29) into Eq. (14), the expression for the inverse quality factor to calculate TED in beam resonators is finally derived as:

$$Q^{-1} = \frac{6\left(1 - \frac{k^*\tau}{k}\right)\Delta_E}{\Omega^2\xi^2} \times \left[\left\{1 + \frac{1 + cos(\xi\zeta)cosh\left(\frac{\xi a_2}{\zeta}\right)}{\left[cos(\xi\zeta) + cosh\left(\frac{\xi a_2}{\zeta}\right)\right]^2} - \frac{3\zeta\left(\zeta^2 sin(\xi\zeta) + a_2 sinh\left(\frac{\xi a_2}{\zeta}\right)\right)}{\xi\left(\zeta^4 + a_2^2\right)\left[cos(\xi\zeta) + cosh\left(\frac{\xi a_2}{\zeta}\right)\right]}\right\}^2 + \left\{\frac{sin(\xi\zeta)sinh\left(\frac{\xi a_2}{\zeta}\right)}{\left[cos(\xi\zeta) + cosh\left(\frac{\xi a_2}{\zeta}\right)\right]^2} + \frac{3\zeta\left(a_2 sin(\xi\zeta) - \zeta^2 sinh\left(\frac{\xi a_2}{\zeta}\right)\right)}{\xi\left(\zeta^4 + a_2^2\right)\left[cos(\xi\zeta) + cosh\left(\frac{\xi a_2}{\zeta}\right)\right]}\right\}^2\right]^{\frac{1}{2}} \tag{30}$$

6. Numerical results

In the previous section, the explicit formula of the Q-factor for TED is derived as Q^{-1}/Δ_E by applying the entropy generation approach. The present work aims to investigate the TED in beam resonators based on

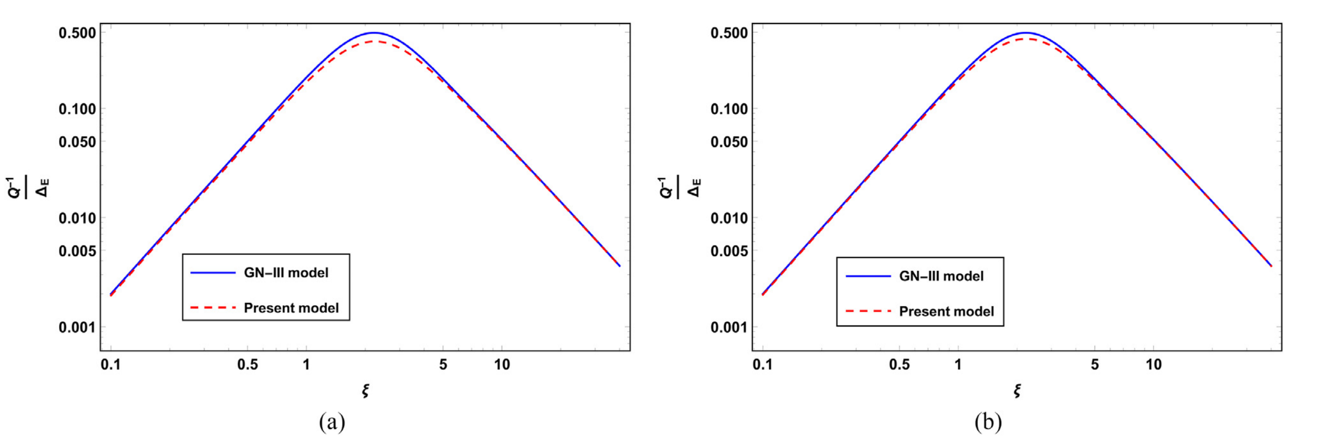

Fig. 2. Variation of Q^{-1}/Δ_E versus non-dimensional frequency ξ for fixed $k^* = 90$ and aspect ratio (a) $L/h = 25$ and (b) $L/h = 30$.

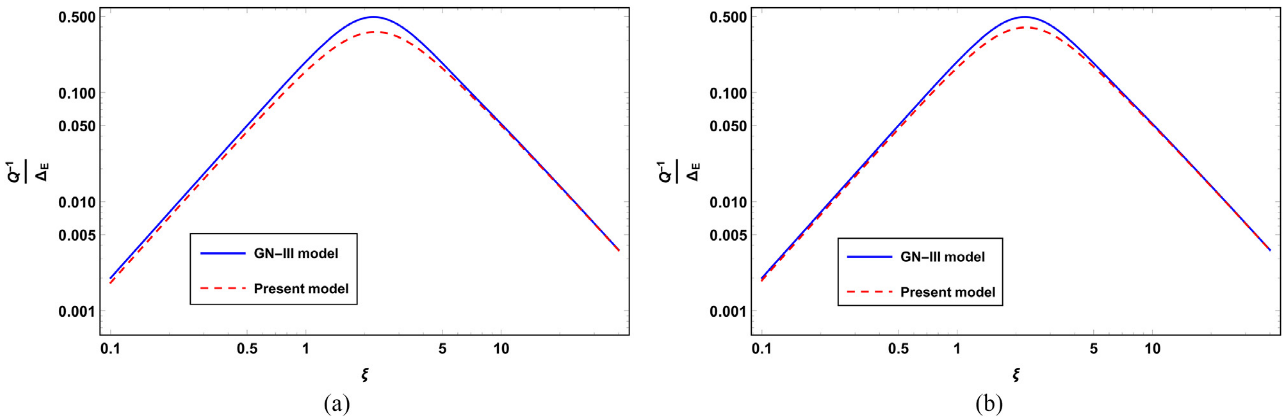

Fig. 3. Variation of Q^{-1}/Δ_E versus non-dimensional frequency ξ for fixed $k^* = 156$ and aspect ratio (a) $L/h = 25$ and (b) $L/h = 30$.

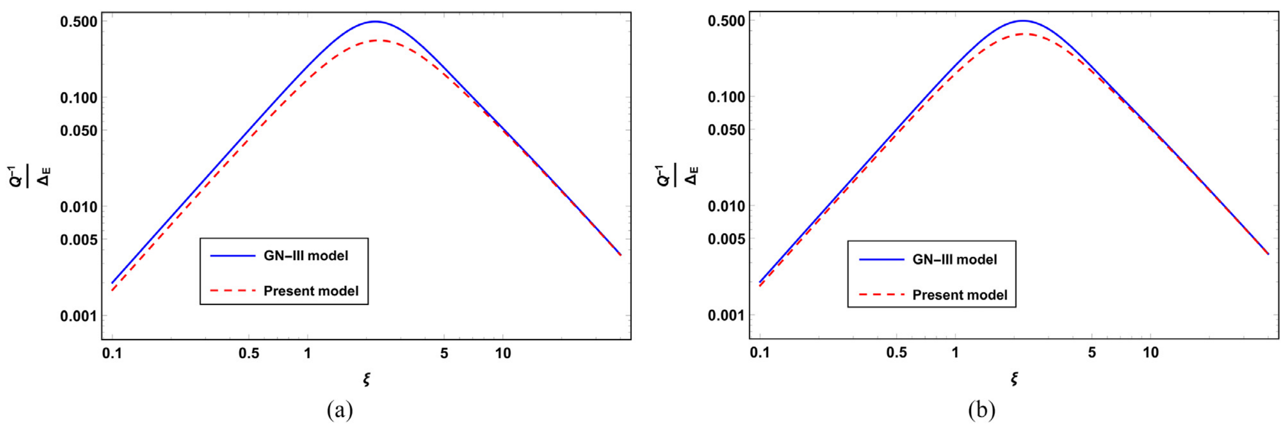

Fig. 4. Variation of Q^{-1}/Δ_E versus non-dimensional frequency ξ for fixed $k^* = 200$ and aspect ratio (a) $L/h = 25$ and (b) $L/h = 30$.

the modified heat conduction equation with a single delay term proposed by Quintanilla [65]. The results of the present model are compared to the corresponding results of the thermoelasticity theory of type GN-III. The effects of some parameters on the TED such as aspect ratio, beam thickness, and dimensionless frequency, are studied. Furthermore, the effects of material constant k^* (conductivity rate) on the Q-factor for TED is also discussed. Here, the material of the beam is selected as Silicon. The properties of Silicon material are listed below [46,64]:

$T_0 = 293\,\text{K},\ E = 169\,\text{GPa},\ \rho = 2330\,\text{Kg/m}^3,\ \nu = 0.22,\ k = 156\,\text{W/mK},$ $C_v = 1.64\times10^6\,\text{J/m}^3\,\text{K},\ \alpha_T = 2.6\times10^{-6}\,\text{K}^{-1}$ and $\tau = 1.72\times10^{-12}\text{s}.$

Figs. 2,3,4 show the variation of thermoelastic damping Q^{-1}/Δ_E (scaled by the relaxation strength Δ_E) with dimensionless frequency, ξ for various aspect ratios in the contexts of the present model and GN-III model. We show the results for the cases when the aspect ratio $L/h = 25$ and $L/h = 30$. Figs. 2–4 also depict the effects of the material parameter (conductivity rate), k^* on TED. This parameter is the characteristic of the present model and GN-III model. In the graphs, two curves show the results for TED associated with GN-III model and the present thermoelasticity model involving a single delay term parameter. As shown in these Figures, the method based on entropy generation is almost close to the curve of the GN-III model for the high-frequencies range. In the case of both the models, the peak value of TED occurs nearly for $\xi \simeq 2.224$. It has been observed that TED increases to a maximum peak value as the frequency increases and decreases after reaching the peak value. The peak value is for the configuration on which the lost energy is the highest. It can be concluded that the difference between the prediction of Q-factor by two models decreases as we increase the aspect ratio of the beam. Therefore, for large aspect ratio, the Q-factor is almost the same for both the models. Furthermore, for large frequencies with a fixed aspect ratio L/h, the errors are negligible. It is further observed that the present model offers the high-quality factor for small aspect ratio in comparison to GN-III model. From the Figures, the effects of material constant k^* on TED can be observed to be very much prominent, implying that there is a significant difference in the prediction of Q-factor by the present model as compared to the GN-III model. When the material constant k^* is smaller than thermal conductivity k, the Q-factor decreases, and when it is greater or equal to k, the Q-factor increases from GN-III model. In all cases, the results of the Q-factor for TED obtained by the present model are better than those shown by GN-III model.

In Fig. 5, the effects of time delay parameter (τ) are depicted for fixed aspect ratio $L/h = 30$ against the normalized frequency. It has been ob-

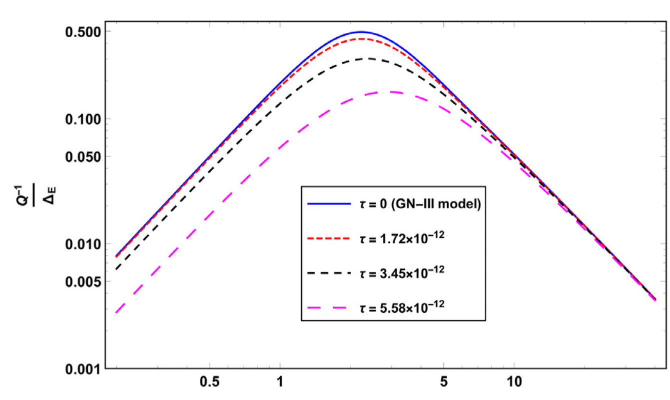

Fig. 5. Effects of time delay parameter on Q^{-1}/Δ_E versus non-dimensional frequency ξ for fixed $k^* = 90$ and aspect ratio $L/h = 30$.

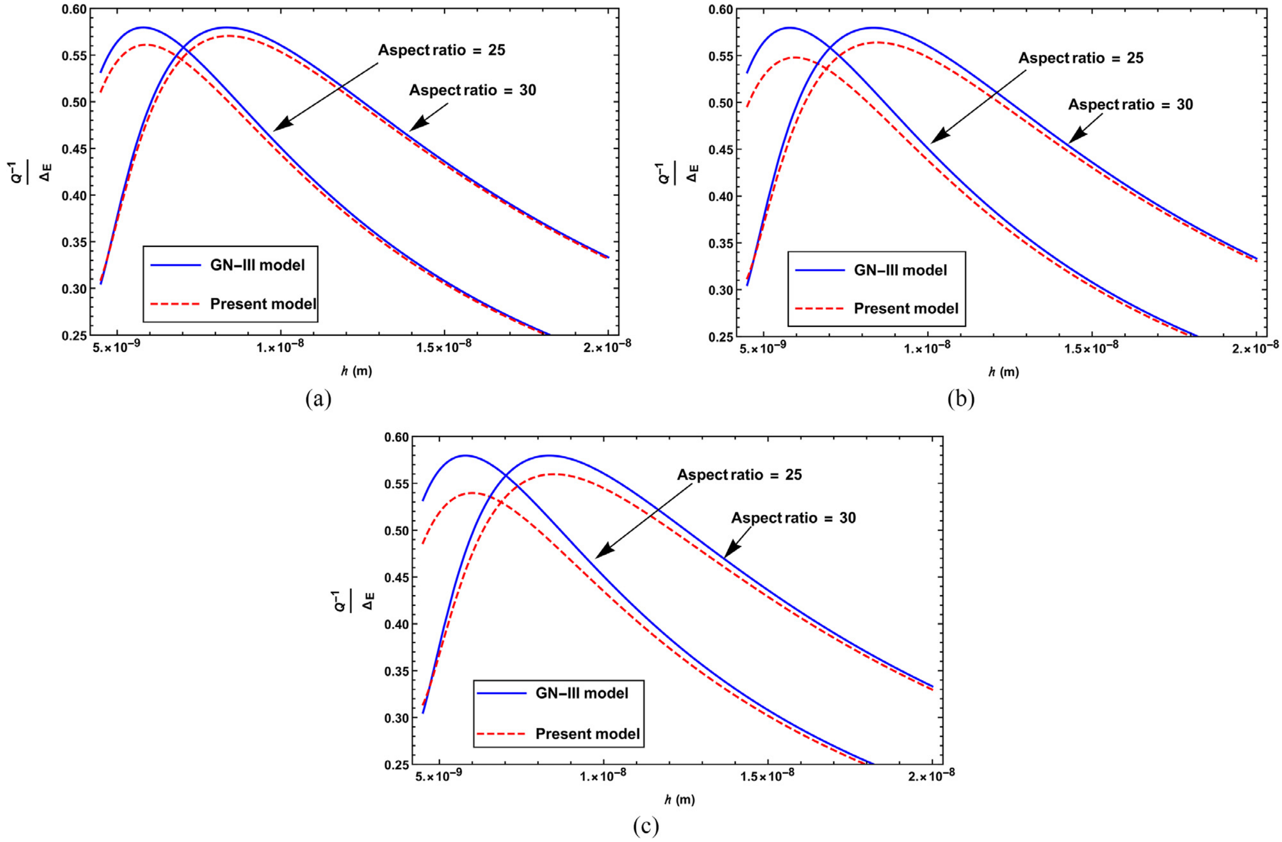

Fig. 6. Variation of Q^{-1}/Δ_E versus beam thickness h for (a) $k^* = 90$, (b) $k^* = 156$, and (c) $k^* = 200$.

served that with the increase in the values of delay time, the Q-factor increases in comparison to the Q-factor predicted by GN-III model. Hence, we can obtain the high Q-factor of the beam resonator. Moreover, TED can occur for a longer time.

Figs. 6 (a,b,c) display the variation of thermoelastic damping Q^{-1}/Δ_E (scale by the relaxation strength Δ_E) for different aspect ratios ($L/h = 25$ and $L/h = 30$) of the beam with respect to beam thickness at nanometer scale. From these figures, one can also observe the effects of material constant k^* on TED. Here, we have considered three cases i.e., when $k^* < k$, $k^* = k$, and $k^* > k$. It is noticed that the difference of peak value in the Q-factor is larger for smaller aspect ratio associated with present and GN-III models. Also, with the increase of aspect ratio, the peak value decreases. From these Figures, it is clear that when we increase aspect ratio, the value of the Q-factor decreases. Furthermore, it is found that the value of the Q-factor in present model is greater than GN-III model and hence, a lower rate of energy loss relative to the stored energy of the resonator can be achieved by applying the present model. Therefore, this resonator with high-quality factor has low damping so that they ring or vibrate for longer duration of time. As observed from Fig. 6 (a,b,c), when we increase the value of material constant k^*, TED decreases and hence, in this case, we can obtain high-value of the Q-factor of the beam resonator.

Fig. 7 depicts the influence of the thickness of the beam resonator on TED for different values of time delay parameter and for aspect ratios

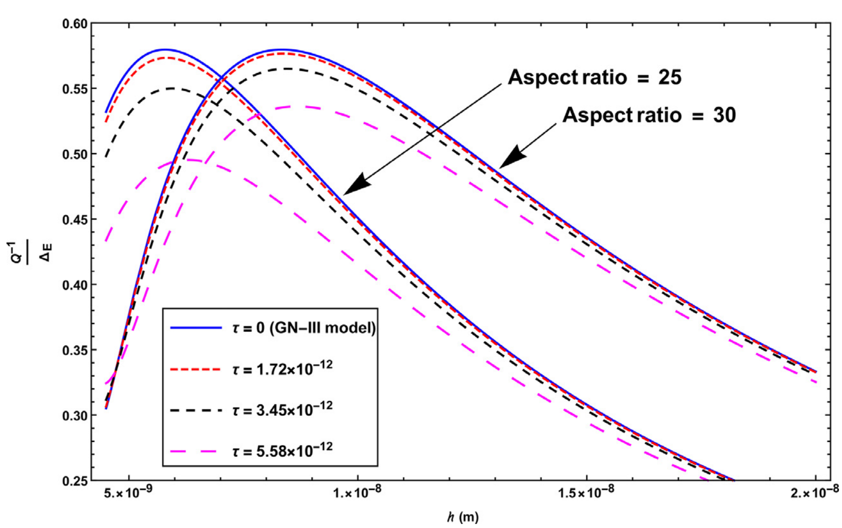

Fig. 7. Variation of Q^{-1}/Δ_E versus beam thickness h for fixed $k^* = 90$ and for different aspect ratios $L/h = 25$ and $L/h = 30$.

$L/h = 25$ and $L/h = 30$. Here we consider $k^* = 90$. We note that there is a prominent effect of the time delay parameter on TED, implying that there is a significant difference in predictions of Q-factor by the present model as compared to GN-III model. It is observed that by increasing the value of delay time, the peak value diverges from GN-III model for the small thickness of beam resonator. In this case, TED decreases, which indicates that the value of the Q-factor increases. Also, it can be seen that the results under the present model converge to the results under GN-III model only for the larger thickness of the beam. However, the present model offers high-quality factor at nanometer scale. This is believed to be an important observation of the present study. It must be mentioned that our results for GN-III model matches with the corresponding results reported by Kumar et al. [23] and Kumar et al.[64].

7. Conclusion

The present work demonstrates the prediction of the quality factor of TED in micro and nano-beam resonators on the basis of the heat conduction model with a single delay term proposed by Quintanilla [65]. To derive the expression of the inverse quality factor for TED, the entropy generation approach method has been used. The quality factor is obtained by calculating the energy dissipated per cycle of vibration over the volume of the beam resonator. The influences of beam thickness, aspect ratio, and dimensionless frequency on the quality factor for TED are investigated in a detailed way. Furthermore, the effects of material constant k^* (conductivity rate) on TED is also discussed. The results of the present model are compared to the corresponding results obtained for GN-III model. The main highlights from the present investigation are outlined as follows:

- The prediction of the quality factor by the present model is higher as compared to the prediction by GN-III model.
- The higher value of the quality factor of the present model can be observed only at the nanoscale, while the quality factor remains approximately the same as GN-III model at the microscale.
- The high-quality factor can also be obtained for higher values of the material constant, k^*.
- Furthermore, higher is the value of relaxation time τ, higher is the quality factor, so that minimum is the energy dissipation.

Declaration of Competing Interest

The authors certify that they have NO affiliations with or involvement in any organization or entity with any financial interest (such as honoraria; educational grants; participation in speakers' bureaus; membership, employment, consultancies, stock ownership, or other equity interest; and expert testimony or patent-licensing arrangements), or non-financial interest (such as personal or professional relationships, affiliations, knowledge or beliefs) in the subject matter or materials discussed in this manuscript.

Acknowledgment

One of the authors (Harendra Kumar) who acknowledges the full financial assistance as SRF fellowship (File No.: 09/1217 (0014)/2017-EMR-1) under Council of Scientific and Industrial Research (CSIR) India to carry out this work.

References

[1] Zhong ZY, Zhou JP, Zhang HL. Thermoelastic damping in functionally graded microbeam resonators. IEEE Sensors J 2017;17:3381–90.
[2] Zotov SA, Simon BR, Prikhodko IP, Trusov AA. Shkel AM. Quality factor maximization through dynamic balancing of tuning fork resonator. IEEE Sensors J 2014;8:2706–14.
[3] Kim SB, Kim JH. Quality factors for the nano-mechanical tubes with thermoelastic damping and initial stress. J Sound Vib 2011;330:1393–402.
[4] Metcalf TH, Pate BB, Photiadis DM, Houston BH. Thermoelastic damping in micromechanical resonators. Appl Phys Lett 2009;95:061903.
[5] Lifshitz R, Roukes ML. Thermoelastic damping in micro- and nanomechanical systems. Phys Rev B 2000;61:5600–9.
[6] Hao Z, Xu Y, Durgam SK. A thermal-energy method for calculating thermoelastic damping in micromechanical resonators. J Sound Vib 2009;322:870–82.
[7] Basak A, Nandakumar K, Chatterjee A. Decoupled three-dimensional finite element computation of thermoelastic damping using zener's approximation. Meccanica 2010;46:371–81.
[8] Vallabhaneni AK, Rhoads JF, Murthy JY, Ruan X. Observation of nonclassical scaling laws in the quality factors of cantilevered carbon nanotube resonators. J Appl Phys 2011;110:034312.
[9] Jiang H, Yu MF, Liu B, Huang Y. Intrinsic energy loss mechanisms in a cantilevered carbon nanotube beam oscillator. Phys Rev Lett 2004;93:185501.
[10] Zener C. Internal friction in solids. I. Theory of internal friction in reeds. Phys Rev 1937;52:230–5.
[11] Zener C. Internal friction in solids II. General theory of thermoelastic internal friction. Phys Rev 1938;53:90–9.
[12] Green AE, Naghdi PM. A re-examination of the base postulates of thermomechanics. Proc R Soc Lond A 1991;432:171–94.
[13] Green AE, Naghdi PM. On undamped heat waves in an elastic solid. J Therm Stress 1992;15:253–64.
[14] Green AE, Naghdi PM. Thermoelasticity without energy dissipation. J Elast 1993;31:189–209.
[15] Kinra VK, Milligan KB. A second-law analysis of thermoelastic damping. J Appl Mech 1994;61:71.
[16] Tai YP, Li P, Zuo WL. An entropy based analytical model for thermoelastic damping in micromechanical resonators. Appl Mech Mater 2012;159:46–50.
[17] Tai Y, Li P. An analytical model for thermoelastic damping in microresonators based on entropy generation. J Vib Acoust 2014;136. 031012–1-8
[18] Zhou HY, Li P, Fang YM. Thermoelastic damping in circular cross-section micro/nanobeam resonators with single-phase-lag time. Int J Mech Sci 2018;142:583–94.
[19] Khisaeva ZF, Ostoja-Starzewski M. Thermoelastic damping in nanomechanical resonators with finite wave speeds. J Therm Stress 2006;29:201–16.
[20] Bostani M, Karami Mohammadi A. Thermoelastic damping in microbeam resonators based on modified strain gradient elasticity and generalized thermoelasticity theories. Acta Mech 2017;228:1–20.
[21] Guo FL, Wang GQ, Rogerson GA. Analysis of thermoelastic damping in micro-and nanomechanical resonators based on dual-phase-lagging generalized thermoelasticity theory. Int J Eng Sci 2012;60:59–65.
[22] Tzou DY. A unified approach for heat conduction from macro to micro-scales. J Heat Transf 1995;117:8–16.
[23] Kumar R, Kumar R, Kumar H. Effects of phase-lag on thermoelastic damping in micromechanical resonators. J Therm Stress 2018;41(9):1115–24. 2
[24] Choudhuri SR. On a thermoelastic three-phase-lag model. J Therm Stress 2007;30(3):231–8. 30
[25] Zamanian M, Khadem SE. Analysis of thermoelastic damping in microresonators by considering the stretching effect. Int J Mech Sci 2010;52(10):1366–75. 1
[26] Guo X, Yi YB, Pourkamali S. A finite element analysis of thermoelastic damping in vented MEMS beam resonators. Int J Mech Sci 2013;74:73–82. 1
[27] Parayil DV, Kulkarni SS, Pawaskar DN. Analytical and numerical solutions for thick beams with thermoelastic damping. Int J Mech Sci 2015;94:10–19. 1
[28] Rezazadeh M, Tahani M, Hosseini SM. Thermoelastic damping in a nonlocal nano-beam resonator as NEMS based on the type III of green–naghdi theory (with energy dissipation). Int J Mech Sci 2015;92:304–11. 1
[29] Parayil DV, Kulkarni SS, Pawaskar DN. A generalized model for thermoelastic damping in beams with mid-plane stretching nonlinearity. Int J Mech Sci 2018;135:582–95. 1
[30] Zhou H, Li P, Fang Y. Thermoelastic damping in circular cross-section micro/nanobeam resonators with single-phase-lag time. Int J Mech Sci 2018;142:583–94. 1
[31] Youssef HM, Alghamdi NA. Thermoelastic damping in nanomechanical resonators based on two-temperature generalized thermoelasticity theory. J Therm Stress 2015;38(12):1345–59. 2
[32] Chen S, Song J, Guo F. Evaluation of thermoelastic damping in micromechanical resonators with axial pretension: an analytical model accounting for two-dimensional thermal conduction. J Therm Stress 2019;22:1–4.
[33] Guo FL, Jiao WJ, Wang GQ, Chen ZQ. Distinctive features of thermoelastic dissipation in microbeam resonators at nanoscale. J Therm Stress 2016;39(3):360–9. 3
[34] Sharma JN. Thermoelastic damping and frequency shift in micro/nanoscale anisotropic beams. J Therm Stress 2011;34(7):650–66. 1
[35] Zhang H, Kim T, Choi G, Cho HH. Thermoelastic damping in micro-and nanomechanical beam resonators considering size effects. Int J Heat Mass Transf 2016;103:783–90. 1
[36] Zhang H, Kim S, Choi G, Xie D, Cho HH. Effect of temperature dependent material properties on thermoelastic damping in thin beams. Int J Heat Mass Transf 2019;139:1031–6. 1
[37] Kumar R, Kumar R. Effects of phase lags on thermoelastic damping in micro-beam resonators. Int J Struct Stability Dyn 2019;31.
[38] Kumar R, Kumar R. A study of thermoelastic damping in micromechanical resonators under unified generalized thermoelasticity formulation. Noise Vib Worldwide 2019;5. 0957456519853814
[39] Zuo W, Li P, Zhang J, Fang Y. Analytical modeling of thermoelastic damping in bilayered microplate resonators. Int J Mech Sci 2016;106:128–37. 1
[40] Fang Y, Li P, Zhou H, Zuo W. Thermoelastic damping in rectangular microplate resonators with three-dimensional heat conduction. Int J Mech Sci 2017;133:578–89. 1

[41] Liu S, Sun Y, Ma J, Yang J. Theoretical analysis of thermoelastic damping in bilayered circular plate resonators with two-dimensional heat conduction. Int J Mech Sci 2018;135:114–23. 1
[42] Zuo W, Li P, Du J, Huang J. Thermoelastic damping in trilayered microplate resonators. Int J Mech Sci 2019;151:595–608. 1
[43] Ma C, Chen S, Guo F. Thermoelastic damping in micromechanical circular plate resonators with radial pre-tension. J Therm Stress 2019;16:1–6.
[44] Fang Y, Li P, Wang Z. Thermoelastic damping in the axisymmetric vibration of circular microplate resonators with two-dimensional heat conduction. J Therm Stress 2013;36(8):830–50. 3
[45] Wang L, Li X, Pan W, Yang Z, Xu J. Analysis of thermoelastic damping in bilayered rectangular microplate resonators with three-dimensional heat conduction. J Mech Sci Technol 2019;33(4):1769–84. 1
[46] Li P, Fang Y, Hu R. Thermoelastic damping in rectangular and circular microplate resonators. J Sound Vib 2012;331(3):721–33. 30
[47] Hossain ST, McWilliam S, Popov AA. An investigation on thermoelastic damping of high-q ring resonators. Int J Mech Sci 2016;106:209–19. 1
[48] Tai Y, Chen N. Thermoelastic damping in the out-of-plane vibration of a microring resonator with rectangular cross-section. Int J Mech Sci 2019;151:684–91. 1
[49] Zhou H, Li P, Fang Y. Single-phase-lag thermoelastic damping models for rectangular cross-sectional micro-and nano-ring resonators. Int J Mech Sci 2019;3:105132.
[50] Tai Y, Li P, Zheng Y, Tian J. Entropy generation and thermoelastic damping in the in-plane vibration of microring resonators. Entropy 2019;21(7):631.
[51] Hossain ST, McWilliam S, Popov AA. An investigation on thermoelastic damping of high-q ring resonators. Int J Mech Sci 2016;106:209–19. 1
[52] Tai Y, Chen N. Thermoelastic damping in the out-of-plane vibration of a microring resonator with rectangular cross-section. Int J Mech Sci 2019;151:684–91. 1
[53] Li P, Fang Y, Zhang J. Thermoelastic damping in microrings with circular cross-section. J Sound Vib 2016;361:341–54. 20
[54] Park SK, Gao XL. Bernoulli–euler beam model based on a modified couple stress theory. J Micromech Microeng 2006;16(11):2355. 15
[55] Kong S, Zhou S, Nie Z, Wang K. Static and dynamic analysis of micro beams based on strain gradient elasticity theory. Int J Eng Sci 2009;47(4):487–98. 1
[56] Kong S, Zhou S, Nie Z, Wang K. The size-dependent natural frequency of bernoulli–euler micro-beams. Int J Eng Sci 2008;46(5):427–37. 1
[57] Rezazadeh G, Vahdat AS, Tayefeh-rezaei S, Cetinkaya C. Thermoelastic damping in a micro-beam resonator using modified couple stress theory. Acta Mechanica 2012;223(6):1137–52. 1
[58] Şimşek M, Reddy JN. Bending and vibration of functionally graded microbeams using a new higher order beam theory and the modified couple stress theory. Int J Eng Sci 2013;64:37–53. 1
[59] Kakhki EK, Hosseini SM, Tahani M. An analytical solution for thermoelastic damping in a micro-beam based on generalized theory of thermoelasticity and modified couple stress theory. Appl Math Model 2016;40(4):3164–74. 15
[60] Borjalilou V, Asghari M, Bagheri E. Small-scale thermoelastic damping in micro-beams utilizing the modified couple stress theory and the dual-phase-lag heat conduction model. J Therm Stress 2019;1:1–4.
[61] Zhong ZY, Zhang WM, Meng G, Wang MY. Thermoelastic damping in the size-dependent microplate resonators based on modified couple stress theory. J Microelectromech Syst 2014;24(2):431–45. 9
[62] Tsiatas GC. A new kirchhoff plate model based on a modified couple stress theory. Int J Solids Struct 2009;46(13):2757–64. 15
[63] Zhong ZY, Zhang WM, Meng G, Wang MY. Thermoelastic damping in the size-dependent microplate resonators based on modified couple stress theory. J Microelectromech Syst 2014;24(2):431–45. 9
[64] Kumar H, Mukhopadhyay S. Analysis of the quality factor of micro-beam resonators based on heat conduction model with a single delay term. J Therm Stress 2019;18:1–4.
[65] Quintanilla R. Some solutions for a family of exact phase-lag heat conduction problems. Mech Res Commun 2011;38:355–60.
[66] Guo FL. Thermo-elastic dissipation of microbeam resonators in the framework of generalized thermos-elasticity theory. J Therm Stress 2013;36:1156–68.
[67] Yourgrau W, der Merwe A, Raw G. Treatise on irreversible and statistical thermodynamics: an introduction to nonclassical thermodynamics. North Chelmsford: Courier Corporation; 2013.